SIXTH EUROPEAN ROTORCRAFT AND POWERED LIFT AIRCRAFT FORUM

Paper No. 27

CO-AXIAL ROTOR AERODYNAMICS IN HOVER

M.J. Andrew

University of Southampton
United Kingdom

September 16-19, 1980
Bristol, England

THE UNIVERSITY, BRISTOL, BS8 1HR, ENGLAND

CO-AXIAL ROTOR AERODYNAMICS IN HOVER

M.J. Andrew
Department of Aeronautics & Astronautics
University of Southampton
United Kingdom

SUMMARY

A prototype remotely piloted co-axial contra-rotating twin rotor (CCTR) helicopter designed by Westland Helicopters Limited and extensively modified for research was used to investigate CCTR aerodynamics in hover. Experimental induced downwash distributions and overall rotor performances are compared with a theoretical model based on momentum, blade element and vortex theories. Good agreement between measured data (comparisons with present rig and results published from a full-scale CCTR are included) and theoretical predictions has been found. Semi-empirical equations have been derived for the initial viscous vortex core size and maximum swirl velocities. The modelling compares favourably with a number of other published results from fixed and rotating blade measurements.

In the past a CCTR has often been misleadingly compared with one of its own rotors. Although this comparison has rendered the CCTR a less inefficient system, it is considered false, in that the single rotor is thrust limited by the onset of blade stall. However, when compared with an equivalent single rotor (same thrust potential) the developed theory indicates that the CCTR layout in hover generates more thrust per unit power because of a reduction in induced power of approximately 5%.

NOTATION

a	lift curve slope
A_r	aspect ratio
b	number of blades
c	blade chord
$\bar{C}_L$	mean lift coefficient
C_{Qi}	induced torque coefficient $Q_i/(\rho V_T^2 \pi R^3)$
C_T	thrust coefficient $T/(\rho V_T^2 \pi R^2)$
K	empirical coefficient
M	Mach number
Q_i	induced torque
r	vortex viscous core radius
R	blade radius
R_t	Reynolds No. based on tip speed and maximum blade thickness
t	maximum blade thickness
T	thrust

v_i strip induced velocity

V_c rotor climb velocity

V_s vortex maximum swirl velocity

V_T rotor tip velocity

V_v total trailing tip vortex wake induced velocity

ω angular velocity of rotor

x distance along blade

α_g blade geometric angle-of-attack

σ_x local blade element solidity

σ rotor solidity

ϕ rotor inflow angle

1. INTRODUCTION

Although a vast amount is now known about single rotor aerodynamics (1) and associated modelling techniques (2,3,4) current knowledge of the flow through a co-axial contra-rotating twin rotor (CCTR) is extremely limited. Even Russian publications fail to disclose concise details of CCTR flow characteristics (5,6).

The objective of this paper is to establish some fundamental properties of a CCTR in hover and to present a computer wake model based on blade element, momentum and vortex theories. One important factor is the model of the tip vortex for which semi-empirical equations have been developed for initial vortex core size and maximum swirl velocity. Roll-up of the viscous core is considered complete as it leaves the trailing edge of the blade tip. The theoretical model assumes that the top rotor of a CCTR behaves as a single rotor while the lower rotor is greatly influenced by the top rotor wake.

CCTR experimental data was obtained from a remotely piloted helicopter, named Mote (7), and designed by Westland Helicopters Limited. The rig was extensively modified for research purposes. To supplement this data, results from a full-scale CCTR test rig (8) are also included, and compared with the developed theory. Although only limited inflight data has been published from the ABC development program (9) it is encouraging to note that the Russian CCTR Ka-25K, flying crane helicopter, is claimed to combine high payload-to-AUW ratio with good manoeuvrability and minimum dimensions (10).

1.1 Rig Characteristics

Configuration	Twin rotor, contra-rotating and co-axially mounted.
No. blades/rotor	Two
Rotor spacing	19.6 cm.
Rotor radius	76 cm.
Chord	5.4 cm.
Twist	None

Blade zero lift angle -1.5°

Lift curve slope (rads) 5.61 (11)

Rigid root.

1.2 Experimental Procedure

The overall lift measurements of the CCTR were recorded from strain gauged supporting flexures while the power consumed by the rotor was deduced from measuring the input power to a driving motor, and correcting for the known motor efficiency characteristics. To ascertain the wake limits of a CCTR extensive smoke visualisation/photography tests were undertaken. Quantitative wake measurements were gathered using non-directional hot wire anemometers and total pressure traverses. Compounding tolerances limit the experimental data to an accuracy of $\pm 8\%$.

2. GENERAL WAKE MODELS

A variety of wake models have been presented to determine the induced downwash distribution along a blade. These include the simple Glauert type strip analysis (12), Fourier series representation of blade airloads (13), local momentum approaches (4, 14) and vortex theories ranging from prescribed wakes (15) to the more advanced free-wake analyses (16). Blade representation by a lifting line has been superseded by the more exacting lifting surface (17) and panel (18) methods.

The combined momentum-blade element approach of strip theory recognises the major design parameters and yields an estimate of the induced velocity at a blade element. However temporal variations in a wake cannot be explained, highlighting the limitations of the theory. Subsequent vortex theories have been developed to provide a more physical representation of the wake and blade airloads, at the expense of increasing computer time. Nevertheless, limitations are still imposed on the models. For example, the most exacting procedure of free-wake analysis is not satisfactory for hover calculations since the wake distortions become so severe that blade vortex interactions are commonly indicated (19). Furthermore the roll-up of a spiralling wake into trailing tip and root vortices is often taken into account by truncating the mesh of trailing and shed vortex elements at an arbitrary wake azimuth station. Both the arbitrary nature of truncation and the debatable point as to whether a well defined root vortex forms, limits the physical validity. Other simplifications include setting the tip vortex strength equal to the peak circulation on the blade and estimating the vortex viscous core size from a direct percentage of blade chord.

2.1 CCTR Wake Approaches

The most fundamental approach to CCTR performance prediction is that reported by Harrington (8). The CCTR is represented by a single rotor with the same radius and an equal number of blades (equivalent blade solidity). The predicted performance for a test CCTR rig shows reasonable agreement over a large thrust range and is therefore a useful model for a first approximation. Another simple CCTR model was utilised in the ABC verification program (20). Employing momentum theory the induced velocity of the lower rotor is assumed to increase by the average downwash from the upper rotor. This is later modified with the supposition

that the upper rotor wake is fully developed and only the inner 50% of the lower rotor is exposed to the fully developed wake; the outer blade sections taking in clean air. Both models are limited by the inadequate representation of the blade loading distribution and consequently over predict rotor torque. Stepneiwski (2) incorporates strip theory into the evaluation of the effect of one rotor on another. Although yielding a better blade loading distribution the effects of wake contraction are disregarded.

A more concise method is that developed by Cheeseman (21) who combined a lifting line approximation to translational lift plus a stream tube model for propeller lift. The inclusion of the helical trailing tip vortices is modelled by a straight line horseshoe vortex system with the tip vortex strengths set equal to the peak circulation of the blade. Wake contraction is not considered. Recently Azuma et al (14) have developed a local momentum theory which can be applied to multi-rotor configurations. Essentially each rotor is treated as a series of wings, each of which has an elliptical circulation distribution. The theory is based on an instantaneous momentum balance of fluid with the blade elemental lift at a local station point in the rotational plane. This theory has led to reasonable results with much less computational time than that required by vortex theory. However, an attenuation coefficient, calculated from approximate vortex theory, has to be introduced to represent the time-wise variation of the local induced velocities following a blade passage. This coefficient is further simplified in certain calculations by treating it as a constant throughout the disc (14).

3. CCTR VORTEX-STRIP THEORY

The aforementioned theories all supplement each other to the extent that an optimum theory should consider the advantages of the various momentum, blade element and vortex approaches. The present theory uses a simplified method with this underlying aim.

Strip theory yields an initial estimate of the induced downwash at a blade element viz:-

$$v_i = \left(\frac{V_c}{2} + \frac{\sigma_x a\omega R}{16}\right)\left(-1 + \left(1 + \frac{2(\alpha_g x\omega - V_c)}{\frac{4V_c^2}{\sigma_x a\omega R} + V_c + \frac{\sigma_x a\omega R}{16}}\right)^{\frac{1}{2}}\right) \qquad (1)$$

Traditionally a tip loss factor is introduced to allow for the finite span of the blade and the associated formation of the tip vortex. Such tip loss factors confusingly truncate the blade radius so that in the tip region no lift is generated. In reality the 'tip loss' is due to lift impairment resulting from the varying downwash over the complete blade induced by the spiralling helical tip vortex wake propagating from all blades in the rotor. The theory derives this loss factor implicitly by calculating the induced downwash from the tip vortex wake at any specified blade station. For hover, by definition, the vertical ascent velocity V_c, is zero. However in the present theory each blade

element perceives an apparent vertical velocity V_v, from the tip vortex wake. That is, the tip vortex induced velocity V_v, at any blade element replaces V_c in equation (1).

The three-dimensional helical trailing tip vortices are modelled by a series of straight line vortex filaments which follow the empirical prescribed paths reported by Landgrebe (15). The associated induced velocities V_v, outside the viscous core are computed using the Biot-Solvert Law. Inside the viscous core, solid body rotation is assumed with V_v, decreasing from a maximum velocity V_s, at the core edge to zero at the core centre. For the lower rotor, V_v, also has an induced contribution from the upper rotor trailing tip vortices and the strip velocity V_i, which is adjusted for wake contraction. Temporal variations of induced downwash are quickly calculated for any specified point in the rotor disc.

Knowing the total downwash velocity the inflow angle at any blade element may be computed vis:-

$$\phi = \frac{(V_i + V_v)}{\omega \, x/R} \qquad (2)$$

Lift and drag forces are thereafter computed in the usual way using two-dimensional aerofoil characteristics.

For completeness, a knowledge of the maximum swirl velocity and core size of a tip vortex is essential for critical evaluation of the induced velocity variation V_v. The following section lists the pertinent features affecting vortex characteristics and derives semi-empirical equations for vortex core radius r, and maximum swirl velocity V_s.

4. TIP VORTEX PARAMETER EVALUATION

A survey of the literature (22-32) shows a useful body of data on vortex viscous core sizes and maximum swirl velocities for rotating blades, and fixed wings. Initial attempts at correlating the data are marred by the wide variety of conditions such as measuring station point and therefore vortex age, free-stream velocities, blade loading distributions, blade aerofoil characteristics and aspect ratio in both free-flight and wind tunnel tests. However, the most pertinent points resulting from these researches contribute adequate guidance for the modelling of the vortex viscous core radii and maximum swirl velocities.

1) Spivey (22) concluded that tip vortices location and direction on a rotating and non-rotating blade are not affected by centrifugal forces or pressure gradients.

2) Leading on from Spivey's work, Chiger et al (23) deduced that the generated vortex structure from fixed wings and rotating blades should be similar.

3) Flow measurements (24, 25) of a fixed rectangular wing tip evince that the viscous core initially forms at the side of the wing tip and moves over to the top surface in the region of maximum thickness (largest pressure gradient). Thereafter it grows and moves slightly inboard leaving the trailing edge of the wing with a non-symmetric perimeter.

4) If roll-up is defined as a symmetrical tip vortex the process may take many wing-tip chords. However it must be emphasised that the large swirl velocities are induced immediately the core departs from the trailing edge of the wing.

5) Dosanjh et al (26) found that the measured circulation value in a rolled-up tip vortex behind a semi-wing mounted in a wind tunnel was only 58% the peak circulation on the wing. This finding has been endorsed by Cook (27) who found that the circulation in a fully developed vortex from a full-scale rotor blade is less than half the expected value.

From dimensional analysis, and assuming that the vortex swirl velocity V_s, depends on tip pressure (C_L), tip speed V_T, blade thickness t, and the time the vortex core is on the blade ($\sim c/V_T$), the following relationship can be deduced:-

$$\frac{V_s}{V_T} = \left(\frac{t}{c}\,\overline{C_L}\right)^{\frac{1}{2}} \qquad (3)$$

Although this relationship compares favourably with the rotating blade data in Table 1 it under estimates the fixed wing data. The most obvious distinction between the fixed wing and rotating blade which could influence the swirl velocity is the large difference in aspect ratio A_r. Entering this parameter into equation (3) with an empirical constant yields an excellent agreement with the wide collocate of experimental data. Accordingly it is concluded that all the major parameters are incorporated in the modelling equation (4).

$$\frac{V_s}{V_T} = \left(1 + \frac{K}{A_r}\right)\left(\frac{t}{c}\,\overline{C_L}\right)^{\frac{1}{2}} \qquad (4)$$

$K = 6.6$. For a rotating blade in hover $\overline{C_L} = 6C_T/\sigma$ and $A_r = 2R/c$. Rotor aspect ratio is based on disc diameter because it is thought that the root vorticies are not predominant wake structures.

Reviewing the literature for the major parameters on vortex core thickness yields little insight. However, one certainty is that the core radius increases with increasing blade angle-of-attack (29). Furthermore from measurements of core radius taken from smoke visualization photographs for various angles-of-attack (15) it can be concluded that the relationship

Source	Comments	A_r	M	Vortex Position	Experimental V_s/V_T	Approximating V_s/V_T $(\frac{t}{c}\bar{C}_L)^{\frac{1}{2}}$	Approximating V_s/V_T $(1 + \frac{6.6}{A_r})(\frac{t}{c}\bar{C}_L)^{\frac{1}{2}}$	Experimental r/c	Approximating r/c $(\frac{1 - M}{\sqrt{M}})\alpha_g \frac{t}{c}$
Cook (27)	Rotor blade hot wire probe	41	0.53	75° azimuth	0.3	0.29	0.34	0.016	0.013
Simons et al (28)	Rotor blade hot wire probe	54	0.125	300° azimuth	0.23	0.25	0.28	0.05 to 0.075	0.042
Present Author	Rotor blade hot wire probe	28	0.102	120° azimuth	0.3 ± 0.03	0.25	0.31	0.074	0.068
Rorke et al (29)	Fixed wing wind tunnel test hot wire probe	4.2	0.2	2c downstream	0.48	0.22	0.57	0.02 to 0.03	0.018
Zalay (30)	Fixed wing wind tunnel test hot wire probe vorticity meter	5.6	0.133	6.5c downstream	0.6	0.26	0.57	0.03 to 0.05	0.036
Panton et al (31)	Fixed wing free flight hot wire probe	9.2	0.123	39.6c downstream	0.72 +.12 -.25	0.36	0.62	0.046	0.045
Iversen et al (32)	Fixed wing wind tunnel test hot wire probe elliptic tip *based on 92% chord	11.4*	0.135	3.25c downstream	0.42	0.35	0.55	0.050	0.049
Chiger et al (23)	Fixed wing wind tunnel test hot wire probe	5.33	.089	trailing edge	0.37	0.33	0.74	.079	.095

TABLE 1 TRAILING TIP VORTEX DATA

is approximately linear. Knowledge of core formation and its transition to the top surface at the wing at maximum thickness t, adds a further parameter viz:-

$$r = fn(\alpha_g, t, ...)$$

Inserting into this equation combinations of $\bar{C}_L$, A_r, V_s, V_T and Reynolds No. based on blade thickness R_t, did not prove fruitful for all the fixed wing and rotating blade cases. The remaining dominant parameter is Mach No. M, (based on V_T for the rotating blade) and equation (5) renders a fair inter-relationship with all the cases tabulated.

$$\frac{r}{c} \approx \frac{(1 - M)}{\sqrt{M}} \alpha_g \, t/c \qquad (5)$$

This relationship conflicts with Rorke et al conclusion (29) that, among other things, Mach No. has no significant independant effect on the core size. However, scrutinising Fig.10 of Rorke's paper shows a spread of results of ±40% about an interpolated line of core thickness versus time ($\alpha_g = 6^o$). Such a conclusion is accordingly open to question.

The contrasting data is that reported by Chiger et al (23). For a NACA 0015 wing section operating at a geometric angle-of-attack of 12 degrees a much smaller swirl velocity was found. This affect is a possible indication of the onset of blade stall and is a similar trend to that reported by Cook (27) who found a diminished swirl velocity and an increase in vortex core size from a partially stalled rotor blade.

5. PRINCIPAL FEATURES AND FUTURE MODIFICATIONS OF VORTEX-STRIP THEORY

Fig.1 depicts the downwash velocity distributions for a single rotor. The modified strip induced velocity contribution v_i, incorporates the effect of the 'apparent vertical ascent velocity' V_v. The slight depression in the tip vortex induced velocity distribution V_v, at 90% blade radius results from the upwash effect of the previous blade trailing tip vortex. The total theoretical velocity distribution compares well with experimental data. The largest discrepancy in velocities at 85% blade radius seems to originate from the differences in the Landgrebe prescribed vortex paths and reality.

Fig.2 compares the present theory with conventional strip theory. Over the complete blade radius the vortex-strip theory predicts a higher induced downwash with a corresponding reduction in blade angle-of-attack at any specified blade element. The consequent decrement in thrust at any blade station is a measure of the 'finite blade losses' which conventional strip theory attempts to incorporate with an arbitrary tip loss factor.

The prescribed wake paths of both a single rotor and a CCTR in Fig.3 were computed using Landgrebe wake coefficients (15). These coefficients, dependant upon thrust coefficient C_T, and wake azimuth position ψ, indicate a less severe trend than the experimental wake

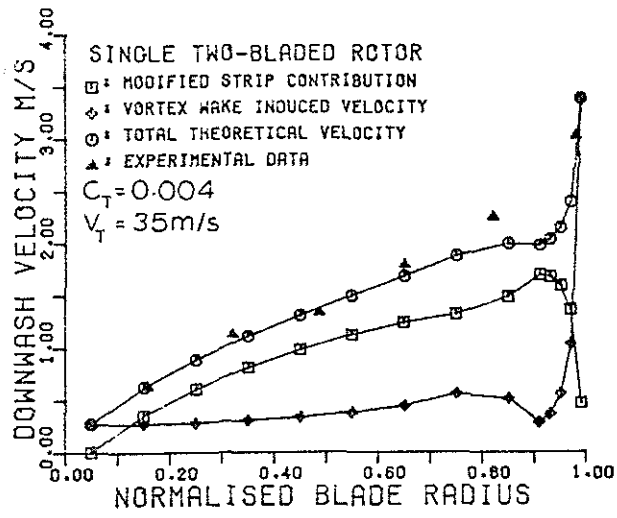

Fig.1 Component Downwash Velocity Distributions

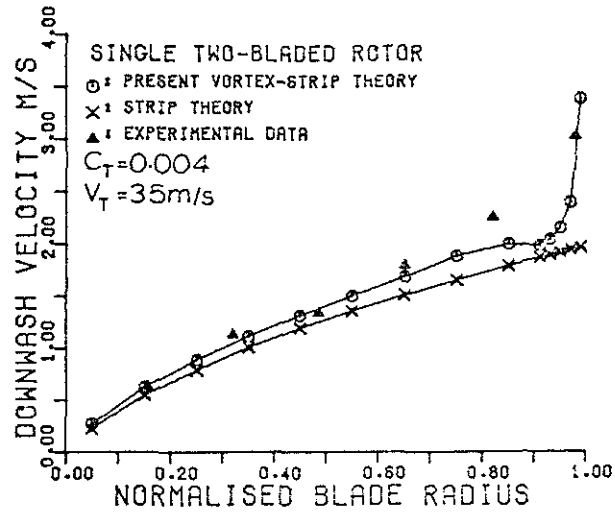

Fig.2 Comparison of Strip and Vortex-Strip Theory

limits. The thrust coefficients of both the upper and lower rotors in the CCTR were computed in an attempt to predict the differing paths taken by the trailing tip vortices from the respective rotors. As can be seen from Fig.3 Landgrebe wake coefficients cannot directly be applied to a CCTR. To allow for this, the Landgrebe prescribed paths will be modified to include the mutual interference of the two wakes. Generally, the mutual affects will result in stronger and weaker contraction of the upper and lower rotor wakes respectively.

Trailing tip vortex decay in a hovering rotor wake is also being investigated and will be included in the wake model in the near future.

5.1 Application of Theory

Fig.4 compares theoretical and experimental performance curves for both CCTR and single rotor models. A further comparison is also made with published results (8) from a full-scale CCTR (Fig.5). Great care is required when comparing single rotors with a CCTR. For a given blade loading, C_T/σ, one rotor of the CCTR generates more thrust per unit torque C_T/C_Q than the CCTR. However, the single rotor is thrust limited by the onset of blade stall and is therefore not a realistic comparison.

A more suitable equivalence is shown in Fig.6 in which the theory was utilised to predict the performance curves of a four bladed single rotor with a blade solidity equal to the CCTR (same thrust potential). In

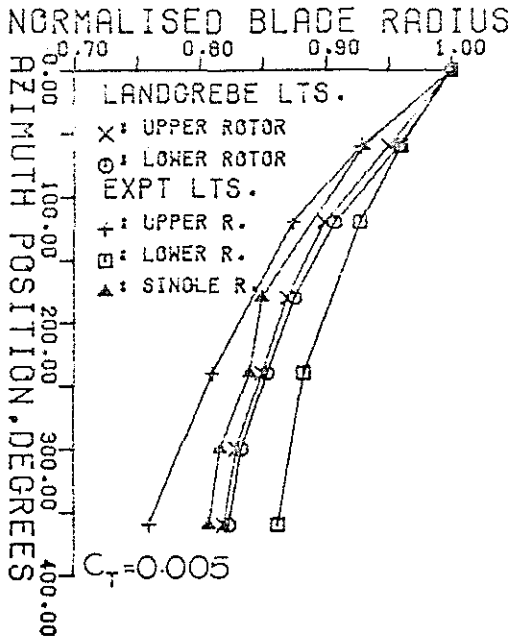

Fig.3 Wake Limits

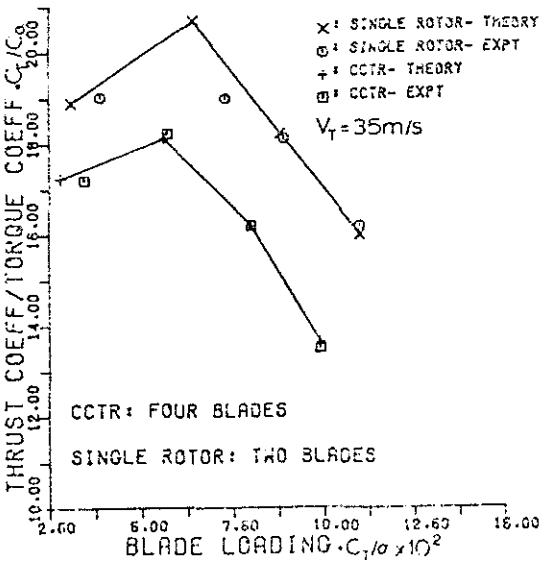

Fig.4 Performance Curves for Mote Rig

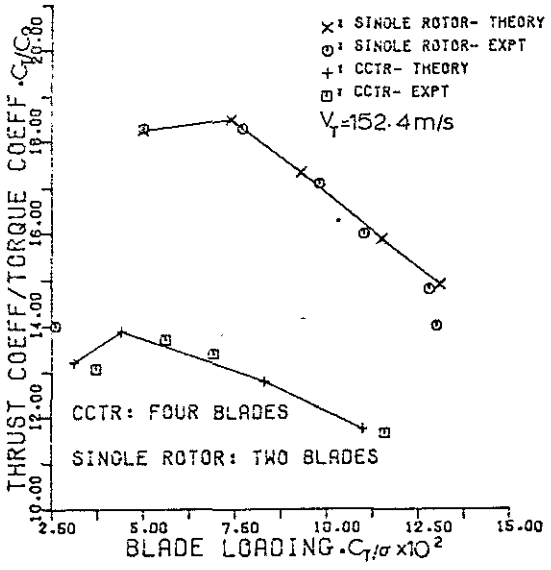

Fig.5 Performance Curves for a Full-Scale CCTR

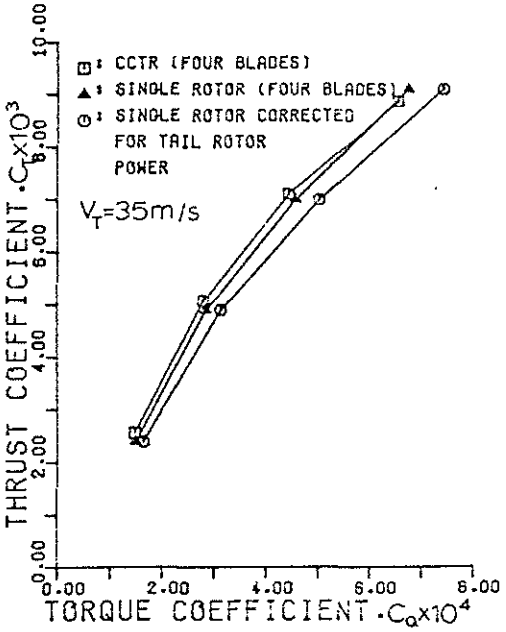

Fig.6 Comparison of Performance Between an Equivalent Single Rotor and a CCTR

this case, for a given blade loading the CCTR generates more thrust per unit torque and results from:-

1) The contraction of the upper wake of a CCTR allows clean air with a slight upwash to be taken by the outboard sections of the lower rotor. Consequently, the effective CCTR disc area increases with a corresponding reduction in induced power. Fig.7 illustrates the relationship between the ratio of thrust coefficient and induced torque coefficient, C_T/C_{Qi}, and blade loading, C_T/σ for the two rotors.

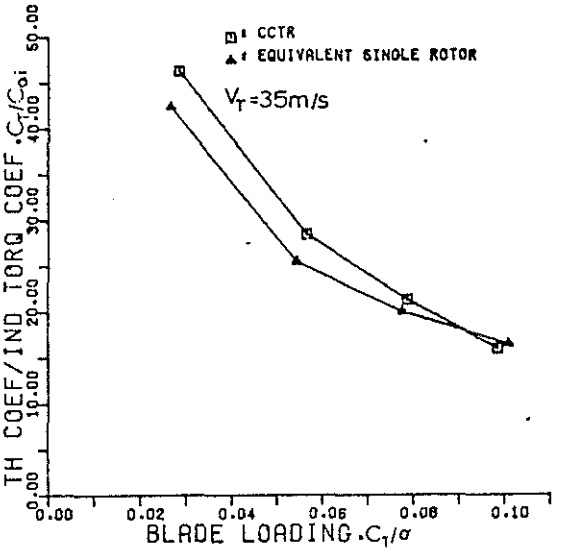

Fig.7 Thrust Coefficient/Induced Torque Coefficient Versus Blade Loading

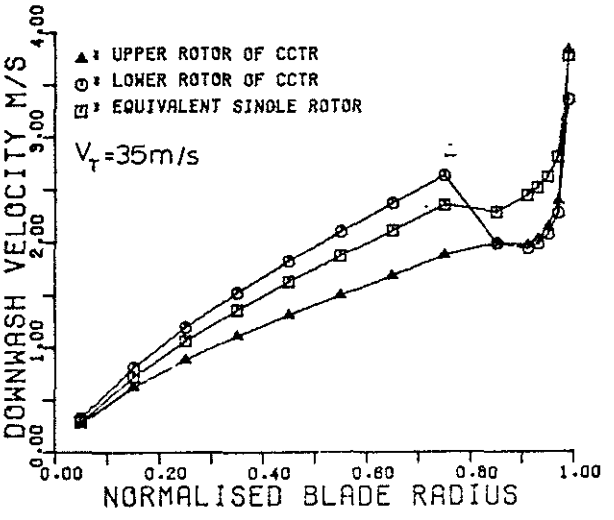

Fig.8 Induced Downwash Distribution

2) Although for a given blade angle-of-attack and tip speed the CCTR generates a stronger tip vortex on the upper rotor, the stack of four spiralling helical tip vortices in the single rotor wake induces a higher total downwash at each blade (Fig.8). By vertically spacing the rotors in the CCTR layout the severity of the degrading vortex induced downwash is lessened.

3) In the trimmed state the CCTR lower rotor thrust is impoverished to 88% of the upper rotor thrust. Alternatively the thrust per blade of the equivalent single rotor is 87% of the thrust produced by each of the CCTR upper rotor blades.

If a further allowance of 10% main rotor power is made for tail rotor power requirements to trim the single rotor then a useful power saving is achieved by employing a CCTR in hover (Fig.6).

The developed theory will continue to be utilised to optimise the CCTR layout for various vertical spacings between rotors, blade aerofoil characteristics and blade tip designs etc.

6. CONCLUSION

1) The conventional Glauert type strip analysis has been modified to incorporate the influence of the trailing helical tip vortices from all blades at any specified blade element. Good agreement between theory and experiment has been found for both model and full-scale rotors. The required computational times are compatible with modern momentum type calculations and are an order of magnitude less than the more advanced vortex theories.

2) Equations for tip vortex maximum swirl velocity V_s, and core radius r, have been derived and favourably compared with a wide range of published results. The equations are:-

$$\frac{V_s}{V_T} = \left(1 + \frac{K}{A_r}\right)\left(\frac{\bar{t}\bar{C}_L}{c}\right)^{\frac{1}{2}} \qquad K = 6.6$$

$$\frac{r}{c} = \left(\frac{1 - M}{\sqrt{M}}\right) \alpha_g \, {}^{t}/_{c}$$

These equations apply to a vortex located at the trailing edge of a blade.

3) The CCTR when compared with an equivalent single rotor (same thrust potential) in trimmed hover produces more thrust per unit torque (Fig.6). Furthermore the CCTR induced power in hover is reduced by approximately 5% that of an equivalent single rotor for the same operating conditions.

ACKNOWLEDGMENTS

The author wishes to thank Professor I.C. Cheeseman for his guidance given in many lengthy discussions on helicopter rotor aerodynamics. Further thanks are extended to Westland Helicopters Limited for supplying the rig and to the Science Research Council for funding the research.

REFERENCES

1. A.R.S. Bramwell — Helicopter Dynamics. Edward Arnold, London 1976.

2. W.Z. Stepniewski — Basic Aerodynamics and Performance of the Helicopter. AGARD-LS-63, 1973.

3. M.C. Cheney
A.J. Landgrebe
Rotor Wakes - Key to Performance Prediction.
AGARD-CP-111, 1972.

4. R. Stricker
W. Gradl
Rotor Prediction with Different Downwash Models.
Fourth European Rotorcraft and Powered Lift Aircraft Forum, Paper No.6, 1978.

5. M.L. Mil et al
Helicopters Calculation and Design Volume I Aerodynamics.
NASATT F-494.

6. V.E. Baskin
L.S. Vil'dgrube
Ye. S. Vozhdayev
G.I. Maykapar
Theory of the Lifting Airscrew.
NASA TT F-823, 1976.

7. J.A. Faulkner
I.A. Simons
The Remotely Piloted Helicopter.
Vertica Vol.1, pp.231-238, 1977.

8. R.D. Harrington
Full-Scale-Tunnel Investigation of the Static-Thrust Performance of a Coaxial Rotor.
NACA TN2318, 1951.

9. A.J. Ruddell
Advancing Blade Concept (ABC^{TM}) Development.
32nd Forum, A.H.S. Forum 1976.

10. J.W.R. Taylor
K. Munson
Jane's All the Worlds Aircraft.
1979-80.

11. F.W. Riegels
Aerofoil Sections.
London, Butterworths 1961.

12. H. Glauert
On the Vertical Ascent of a Helicopter.
ARC R&M No.1132, 1927.

13. K.W. Mangler
H.B. Squire
The Induced Velocity Field of a Rotor.
ARC R&M No.2642, 1953.

14. A. Azuma
K. Kawachi
Local Momentum Theory and its Application to the Rotary Wing.
J. Aircraft Vol.16, No.1, 1979.

15. A.J. Landgrebe
The Wake Geometry of a Hovering Helicopter Rotor and its Influence on Rotor Performance.
28th Forum, A.H.S. 1972.

16. D.R. Clark
A.C. Leiper
The Free Wake Analysis.
25th Forum, A.H.S., 1969.

17. J.D. Kocurek
J.L. Tangler
A Prescribed Wake Lifting Surface Hover Performance Analysis.
32nd Forum, A.H.S., 1976.

18. W. Sent — Higher Order Panel Method Applied to Vorticity-Transport-Equation. 5th European Rotorcraft and Powered Lift Aircraft Forum, Amsterdam, 1979.

19. S.G. Sadler — A Method for Predicting Helicopter Wake Geometry, Wake-Induced Flow and Wake Effects on Blade Airloads. 27th Forum, A.H.S., 1971.

20. V.M. Paglino — Forward Flight Performance of a Coaxial Rigid Rotor. 27th Forum, A.H.S., 1971.

21. I.C. Cheeseman — A Method of Calculating the Effect of One Helicopter Rotor on Another. ARC Tech.Rep. C.P. No.406, 1958.

22. R.F. Spivey — Blade Tip Aerodynamics - Profile and Planform Effects. 24th Forum, A.H.S., 1968.

23. N.A. Chigier, V.R. Corsiglia — Tip Vortices - Velocity Distributions. 27th Forum, A.H.S., 1971.

24. J.D. Hoffman, H.R. Velkoff — Vortex Flow over Helicopter Rotor Tips. J. Aircraft, Vol.8, No.9, 1971.

25. M.S. Francis, D.A. Kennedy — Formation of a Trailing Tip Vortex. J. Aircraft, Vol.16, No.3, 1979.

26. D.S. Dosanjh, E.P. Gaspaek, S. Eskinazi — Decay of a Viscous Trailing Vortex. The Aeronautical Quarterly, May 1962.

27. C.V. Cook — The Structure of a Rotor Blade Tip Vortex. AGARD CP-111, Reference 3.

28. I.A. Simons, R.E. Pacifico, J.P. Jones — The Movement, Structure and Breakdown of Trailing Vortices from a Rotor Blade. CAL/USAA Avlabs Symposium, June 1966.

29. J.B. Rorke, R.C. Moffitt, J.F. Ward — Wind Tunnel Simulation of Full Scale Vortices. 28th Forum, A.H.S., 1972.

30. A.D. Zaly — Hot Wire and Vorticity Meter Wake Vortex Surveys. AIAA Journal, Vol.14, No.5, 1976.

31. R.L. Panton, W.L. Oberkampf, N. Saskic — Flight Measurements of a Wing Tip Vortex. J. Aircraft, Vol.17, No.4, 1980.

32. J.D. Iversen, V.R. Carsiglia, D.R. Backus, R.A. Brickman — Hot-Wire, Laser-Anemometer, and Force Measurements of Interacting Trailing Vortices. J. Aircraft, Vol.16, No.7, 1979.